Biochar

ORIGINAL RESEARCH

Removal of per- and polyfluoroalkyl substances and organic fluorine from sewage sludge and sea sand by pyrolysis

Matěj Hušek[1,2], Jaroslav Semerád[3], Siarhei Skoblia[4], Jaroslav Moško[1,2], Jaroslav Kukla[5], Zdeněk Beňo[4], Michal Jeremiáš[2], Tomáš Cajthaml[3,5], Michael Komárek[6] and Michael Pohořelý[1,2]*

Abstract

Pyrolysis is one method for treating sewage sludge, particularly in remote areas or decentralised systems. The end product of pyrolysis, sludge-char, can serve as a soil improver. However, there is a lack of comprehensive data on the organic pollutants' behaviour in sludge-char. In our work, we focused on the behaviour of per- and polyfluoroalkyl substances (PFASs). Sludge was pyrolyzed at 200–700 °C to determine the minimum safe temperature for effective PFASs removal. It is important to note that PFASs may not only be mineralized but also cleaved to unanalyzed PFASs and other organofluorinated substances. To address this issue, we incorporated additional measurements of organic fluorine in the experiment using combustion ion chromatography (CIC). Due to the inherent heterogeneity of sludge, containing a variety of pollutants and their precursors, we conducted pyrolysis on artificially contaminated sand. This allowed us to assess and compare the behaviour of PFASs in a homogeneous matrix. Based on our analyses, we determined that a temperature greater than 400 °C is imperative for effective PFASs and organic fluorine removal. The results were verified by analyzing samples from a commercial sludge pyrolysis unit at the Bohuslavice-Trutnov WWTP, which confirmed our measurements. In light of these results, it becomes evident that sludge pyrolysis below 400 °C is unsuitable for PFAS removal from sewage sludge.

Highlights

- The minimum temperature for significant PFASs and organic fluorine removal was 400 °C.
- PFASs were part of primary pyrolysis gas: purification or combustion is necessary.
- Contamination by PFASs and their congeners could be monitored with organic fluorine.

Keywords Sewage sludge, PFAS, Pyrolysis, Carbonization, Sludge-char, Organic fluorine

Springer

Graphical Abstract

---

1 Introduction

Per- and polyfluoroalkyl substances (PFASs) are persistent synthetic chemicals with more than 12,000 different species containing carbon–fluorine bonds (EPA 2021). This bond is one of the strongest in organic chemistry; therefore, PFASs are characterised by high chemical and thermal stability and environmental persistence (O'Hagan 2008; Stahl et al. 2011). Depending on the number of carbons in a molecule, PFASs are categorized into long-, short-, and ultrashort-chain groups (Ateia et al. 2019; Buck et al. 2011). PFASs find application in various industrial sectors, such as electroplating, electronics, plastics, firefighting foam, textile impregnation, semiconductors, sports equipment, and pipes due to their different properties, such as low surface tension, non-flammability, hydrophobicity, oleophobicity, or good thermal conductivity (Glüge et al. 2020). However, they can affect the human body's functioning, leading to cancer, changes in sperm quality, cholesterol production, or endocrine gland disruption (Fenton et al. 2021).

Their extensive use results in their spread through waste streams (mainly contaminated water and sewage sludge) into the environment (Munoz et al. 2022; Tavasoli et al. 2021), which can result in their presence in plants and the food chain (Ghisi et al. 2019; Ruan et al. 2015; Semerád et al. 2022). From the available data, the concentration of PFASs (represented by perfluorooctanesulfonic acid (PFOS) and perfluoro-n-octanoic acid (PFOA)) in sewage sludge varies considerably and has been measured in the range of $0.1–1191$ ng g^{-1} (PFOS)

and $0.1–1517$ ng g^{-1} (PFOA), respectively (Hall et al. 2021). Even though some authors have already reported PFASs undergo biodegradation in soil (Horst et al. 2020; Zhang et al. 2022b), given their diverse types and the precautionary principle to protect the soil stock, food chain, and human health, we cannot only rely on the self-cleaning function of soil.

Thus, PFAS-containing sludge should not be used for direct material recovery (agriculture or composting) but treated to remove PFASs and other organic pollutants. From our perspective, thermal treatment methods, such as mono-incineration or pyrolysis, are ways of treating sludge to eliminate present organic pollutants (Hušek et al. 2022). Mono-incineration is a centralized solution for large quantities of sludge, while pyrolysis is more applicable in remote areas with annual sludge production greater than 500 t$_{DM}$. The resulting sludge-char (solid pyrolysis product) finds application in land reclamation as a soil improver, increases soil permeability and water retention, and serves as a medium- to long-term source of phosphorus (Hušek et al. 2022). However, the requirement is a low content of heavy metals in sludge, as they tend to concentrate in char (Mancinelli et al. 2016; Zhang et al. 2021). In the case of organic pollutants during pyrolysis, residence time and operating temperature are crucial (Buss 2021). However, there is currently still legislative distrust of pyrolysis persists due to the wide range of organic pollutants in sewage sludge and the lack of data on their removal, including PFAS (Huygens et al. 2019; Regulation (EU) 2019/1009).

Several authors have described PFAS behaviour and requirements for their removal in pyrolysis (oxygen-free atmosphere). According to Wang et al. (2022), PFASs' thermal decomposition occurs in a gas phase or in/on solids depending on their ability to volatilize. Volatilization is affected by the presence of salts, heterogeneity and consistency of surface/matrix, and pyrolysis temperature. Thermal decomposition is influenced by the functional group and its non-fluorinated part of a chain (if present), the perfluorocarbons' number, reactor type, and reaction atmosphere physicochemical properties. It is also generally affected by temperature, gas content, residence time, and gaseous and solid phases mixing rate (Wang et al. 2022). Alinezhad et al. (2022) mentioned the matter of physical transitions, such as melting and evaporation, and different multistep chemical reactions, such as radical-mediated initiation and chain propagation, recombination, stripping, and termination. Winchell et al. (2021) highlighted the importance of hydrodefluorination in removing PFASs, temperature, reactor design, and residence time. During hydrodefluorination, the C–F bond is converted to a C–H bond, for which sufficient hydrogen is required. Simultaneously, hydrogen is one of the fluorine acceptors and acts as a reagent (catalyst) in the reaction (Winchell et al. 2021). Hydrogen enters the reaction from residual moisture and sludge composition (Moško et al. 2022, 2020). Decomposition is initiated by both end-chain and random-chain scission (Alinezhad et al. 2022). Perfluoroalkyl carboxylic acids (PFCAs) decomposition and defloration start above 150 °C, and over 500 °C leads, among other defloration products, to the formation of volatile organofluorine (VOF – CF_4, C_2F_6, C_2F_4), coke, and cyclic compounds (Wang et al. 2022). For longer-chain PFCAs, pyrolysis products are shorter-chain PFCAs such as 1H-perfluoroalkanes, perfluoro-1-alkenes, CO, CO_2, HF, and unidentified VOF (Wang et al. 2022). By perfluoroalkyl sulfonic acids (PFSAs) – a PFOS representative, the defloration and decomposition only begin above 300 °C (Wang et al. 2022) and are based on HF elimination leading to the formation of α-sultone, which degrades to SO_2 and perfluorooctanoyl fluoride (Weber et al. 2021).

The amount of analyzed PFASs during pyrolysis (in char and soil) decreases with increasing temperature. 500 °C can be considered as the limit below which the pyrolysis operation temperature should not drop (Alinezhad et al. 2022; Kundu et al. 2021; Bamdad et al. 2022; Thoma et al. 2022; Sörengård et al. 2020; McNamara et al. 2022; Williams et al. 2021; Sørmo et al. 2023). However, these publications do not include analyses of organic fluorine (Aro et al. 2021; Kärrman et al. 2021) in char or pyrolyzed soil to rule out the presence of PFAS "dark matter" products (Kotthoff and Bücking 2018): unknown and unanalyzed

PFASs and PFASs cleavage products (McNamara et al. 2022; Sørmo et al. 2023). A mere decrease in the analyzed PFASs content may not indicate their removal but only their transformation. The analysis of organic fluorine provides a control mechanism, but there is still a gap in the research due to the lack of broader determination and demonstration of changes in organic fluorine content. Simultaneously, along with organofluorine from PFASs, organic fluorine contained in other pollutants, such as selected pharmaceuticals and agrochemicals, is also measured (Han et al. 2021).

In our work, we pyrolyzed sewage sludge and artificially contaminated sea sand at 200–700 °C. We aimed to determine the temperature at which the analyzed PFASs drop below the limit of quantification (LOQ), observe the change in organic fluorine content relative to the temperature, and monitor PFAS content leading to the determination of a safe operating temperature for sludge pyrolysis units that effectively remove PFAS, including all organofluorinated substances. Using artificially contaminated sea sand allowed us to simulate an environment without other pollutants and PFAS precursors that could affect the pyrolysis behaviour of the observed PFASs. To distinguish the difference between the behaviour of standard PFASs and PFASs that are part of the sludge matrix. The obtained data were verified on a commercial sludge pyrolysis unit operated at the Bohuslavice-Trutnov wastewater treatment plant (WWTP) in the Czech Republic (CZE) – Additional file 1: Fig. S1.

2 Materials and methods
2.1 Materials
The LC column XSelect CSH C18 (75×2.1 mm, 2.5 μm) and the XSelect CSH C18 (2.5 μm) precolumn were purchased from Waters (USA). Milli-Q water was prepared by a Direct-Q® water purification system (18.2 MΩ. cm^{-1}; Merck, Germany). Methanol for extraction (HPLC grade) was obtained from VWR (Czech Republic), and acetonitrile (LC–MS grade) was purchased from Honeywell Company (USA). The SPE Supelclean™ ENVI-Carb™ columns were obtained from Merck (Germany). The standards of PFAS were purchased as analytical grade chemicals (>97% purity) from Apollo Scientific (UK) or in stock solutions of 10 μg.ml^{-1} from Wellington Laboratories (Canada). GenX (FRD-902) was obtained from HPC Standards (Germany).

2.2 Sample description and preparation for pyrolysis experiment
Before thermal treatment, the sea sand used (Sea Sand Purified CAS: 7631-86-9) was contaminated with 24 different PFASs, including representatives of PFCAs, PFSAs, perfluoroalkane sulfonamides (FASAs), fluorotelomer

acids (FTAs), fluorotelomer sulfonic acids (FTSAs) and 2,3,3,3-tetrafluoro-2-(heptafluoropropoxy)propanoic acid (HFPO-DA), see Additional file 1: Table S1 (PFASs with an asterisk) for detailed information about the individual chemicals. The studied stabilized sewage sludge was chosen according to the content of a wide range of PFASs. The place of origin was WWTP, with a capacity of approximately 30,000 population equivalent (PE), mesophilic anaerobic sludge stabilization, and dewatering of the digested sludge by centrifuge. Subsequently, the sampled sludge was dried to constant moisture in a dry outdoor environment, ground on a cutting mill, and sieved to a fraction of 0.5 to 2.0 mm.

The physical and chemical properties of the sludge and sludge-char are summarised in Additional file 1: Tables S2 and S3. The ash content (A) was determined according to standard ČSN EN 15403 and the volatile content (V) according to ČSN EN 15402. The elementary analysis was performed in a Vario EL Cube (Elementar). The lower heating value (LHV) and higher heating value (HHV) were determined based on ČSN EN 15400. The chlorine and fluorine content of the sample was determined by the analysis of calorimetric vessel leachate after completion of calorimetric analysis following ČSN EN 15408. The solution analysis by ion chromatography was performed on an ICS 1000 (Dionex) instrument. For more information, see Moško et al. (2021b).

The FTIR analysis was performed on a Nicolet iS100 spectrometer (Thermo-Nicolet, USA) in conjunction with a diamond ATR attachment Smart Orbit TM (Thermo-Nicolet, USA), reflectance measurement – DTGS KBr detector. The measurement parameters included spectral range 4000–400 cm^{-1}, resolution 4 cm^{-1}, number of spectral accumulations 64, and Happ-Genzel apodization. Spectra were processed using Omnic 9 software (Thermo-Nicolet Instruments Co., USA). ATR correction and subtraction of air humidity and CO_2 were performed. The portion of the spectra ranging from 2500 to 1900 cm^{-1} was excluded due to the ATR artefact of the crystal. The results are shown in Additional file 1: Fig. S2.

2.3 Thermal treatment – pyrolysis

The samples for pyrolysis were prepared in a stainless steel fixed-bed reactor by slow pyrolysis of approximately 110 g of sea sand or 60 g of dry sewage sludge. The reactor was made of 17251 (US 309) steel tube: 25 mm × 2 mm with a length of 40 cm. The reactor was placed in the electrically heated oven (schematically shown in Fig. 1) and heated to the desired temperature (200, 250, 300, 400, 500, 600, and 700 °C) for 2 h. These chosen temperatures simulate commonly used thermal treatment methods: torrefaction (200–250 °C), low-temperature pyrolysis (< 500 °C), and low-medium temperature pyrolysis (500–700 °C).

Throughout the experiments, including the time before the reactor was placed into the oven and during the reactor's cooling after the experiments, the inert carrier gas – helium – was continuously supplied to the bottom of the reactor at a constant flow rate of 150 ml min^{-1}. The off-gas from the reactor (mixture of carrier gas,
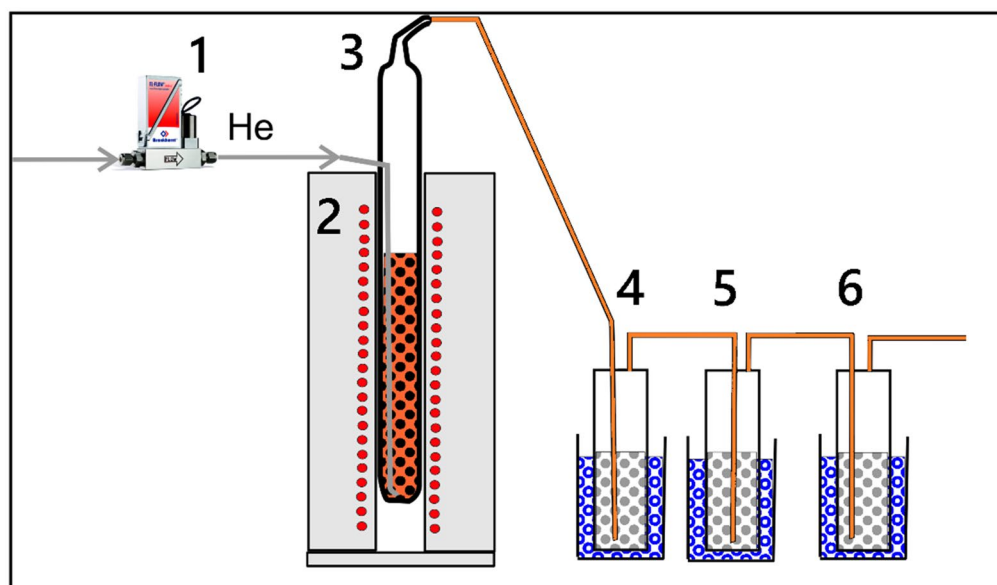
Fig. 1 Scheme of the pyrolysis apparatus: **1** mass flow controller, **2** oven, **3** stainless steel reactor, and **4**–**6** impingers containing acetone and cooled in an ice bath

condensing and non-condensing gases) subsequently passed through three ice-bath cooled impingers containing acetone to trap the condensing part of the off-gas. The non-condensing part was not captured and analyzed. The experimental methodology was adopted and adjusted from our previous work Moško et al. (2021a). The most significant modification is using a steel reactor instead of a quartz reactor to prevent its destruction due to HF release.

2.4 Analysis of PFASs
Five different samples were analyzed for the presence of 37 different PFASs (Additional file 1: Table S1): sea sand, thermally treated sea sand, sewage sludge, sludge-char, and acetone solutions containing absorbed pyrolysis condensate. The PFASs analyzed represented their entire spectrum with respect to the chain length (long and short) and their substitutes (potassium-9-chlorohexadecafluoro-3-oxanonane-1-sulfonate (9Cl-PF3ONS), potassium-11-chloroeicosafluoro-3-oxaundecane-1-sulfonate (11Cl-PF3OUdS), NaDONA (sodium dodecafluoro-3H-4, 8-dioxanonanoate), and HFPO-DA (GenX)). The methodology for analyzing sea sand, sewage sludge, and sludge-chars is consistent with that used in our previous publication by Semerád et al. (2020).

2.4.1 Sample extraction and purification
The artificially contaminated sea sand, sewage sludge, and sludge-char were extracted using previously validated and published method (Semerád et al. 2020). Briefly, within the protocol, solid samples were freeze-dried, greatly homogenized, and extracted by pressurized liquid extraction (PLE) with three cycles of heated methanol (3–5 g, 150 °C and 1500 psi). Afterwards, the obtained extracts were purified using Supelclean™ ENVI-Carb™ columns according to the same publication. Liquid samples, pyrolysis condensates containing acetone as a solvent, were evaporated under a gentle stream of nitrogen and reconstituted in methanol. As in the case of solid sample extracts, these reconstitute condensates were purified equally using the SPE cleaning step prior to the LC–MS/MS analysis.

2.4.2 LC–MS analysis
The quantification of 37 representatives of PFASs has been achieved using the same method and instrumentation as in a previous publication focused on PFAS screening in various matrices (Semerád et al. 2020). Briefly: the LC–MS/MS system consisted of an LC Shimadzu Nexera X2 and Sciex 4500 mass spectrometer operating in negative mode. Targeted PFASs have been separated on a XSelect CSH C18 column (75×2.1 mm, 2.5 µm, Waters, USA) equipped with a pre-column. For each analysis, 5 µl

of the sample was injected into a column heated to 40 °C, using a gradient elution with a flow rate of 0.6 ml.min^{-1} and two solvents A: acetonitrile:formic acid (99.5:0.5) and B: water:acetonitrile:formic acid (79.5:20.0:0.5). The gradient was as follows (min, %A): 0, 80; 0.5, 80; 5, 10; 12, 10; 15, 5; 16, 0; 20, 0; 25, 80; 30, and 80. The detailed settings of the mass spectrometer and limits of detection/quantification are shown in Additional file 1: Tables S4a and S4b. Quality control has been introduced and followed the same structure used in a previous publication (Semerád et al. 2022) to achieve reliable results.

2.5 Fluorine content
Total fluorine (Additional file 1: Chapter S7) and organic fluorine have been determined by combustion ion chromatography (CIC). Total organic fluorine was determined using the direct combustion of solid samples (100 ± 1 mg) weighted into quartz. The organic fluorine was determined in organic extract or acetone condensate as follows. Methanol extract of solid materials obtained by PLE (5–10 g) (sewage sludge, sludge-char, or sand) or acetone condensate were concentrated under a gentle stream of nitrogen, transferred into quartz cups, evaporated to dryness and combusted in a combustion module Xprep C-IC (Trace Elemental Instruments) as solid samples. The gas flow rate was 300 ml.min^{-1} for oxygen and 100 ml.min^{-1} for argon. The temperatures of the furnaces were 750 and 1000 °C. As an absorption solution, 5 ml of hydrogen peroxide (100 mg.l^{-1}) in MQ water has been used. After the combustion, the Dionex™ ICS-5000 Ion Chromatography System (Thermo Scientific) with Dionex AG18 (4×50 mm) guard column and AS18 (4×250 mm) anion exchange column together with suppressed conductivity detection by an ADRS600 dynamically regenerated suppressor were used to determine the concentration of fluorides in absorption solution. The run time of the whole method was 30 min and consisted of elution at a flow rate of 1 ml.min^{-1} and the following gradient: 0–1 min; 10 mM KOH; 1–4 min; from 10 to 23 mM KOH. The mobile phase was prepared by diluting 0.1 M KOH eluent concentrate for ion chromatography (Sigma-Aldrich). The data processing was performed using Chromeleon 7.3 (Thermo Scientific Inc.).

2.6 Data analysis, presentation, mass balance and energy distribution, gas composition, recovery rate, and removal efficiency
The LC–MS/MS data as well as the construction of the calibration curves used for ME determination, were processed by Analyst 1.6.3 software.

The mass balance and energy distribution of the process at 600 °C and gas composition are given in the

Additional file 1: Chapter S5, Tables S5, S6, and S7 and Fig. S3, including comments.

The removal efficiency (RE) of PFASs and organic fluorine by pyrolysis was calculated according to Eq. (1).

$$RE = 100 * \left(1 - \frac{c_{pyr} * m_{pyr}}{c_{sam} * m_{sam}}\right) \qquad (1)$$

where RE is the removal efficiency in %; c_{pyr} is the concentration of the substance of interest (PFASs or organic fluorine) in a pyrolyzed sample in ng.g$^{-1}_{DM}$; m_{pyr} is the mass of the sample after pyrolysis in g; c_{sam} is the concentration of the substance of interest in a sample before pyrolysis in ng g$^{-1}_{DM}$, and m_{sam} is the mass of the sample before pyrolysis in g$_{DM}$.

2.7 Bohuslavice-Trutnov sludge-char properties and pollutants analysis

The ash content (A) and ultimate analysis in Table 6 were performed as with the sludge in Chapter 2.2. The PAHs were determined based on ČSN EN 16181, PCBs on ČSN EN 17322, AOX on ČSN EN 16166, pharmaceuticals and personal care products (PPCP), see Moško et al. (2021a). The methodology for determining the structural properties was adopted from our previous publication by Moško et al. (2021b) using ASAP 2020 and ASAP 2050 automated volumetric gas adsorption instruments (Micromeritics). The phosphorus content was determined according to Unified Work Procedures – SOP 62 A ÚKZÚZ by ICP-OES and converted to P_2O_5. The content of the individual heavy metals in Table 7 was established according to the standards: ČSN EN ISO 5961 – Cd, ČSN ISO 8288 – Pb, ČSN 46 5735 – Hg, ČSN EN ISO 15586 – As, and ČSN EN 1233 – Cr.

3 Results and discussion

The chapter is structured into three parts dealing with artificially contaminated sand, sewage sludge, and the commercial sludge pyrolysis unit of the Bohuslavice-Trutnov WWTP. Changes in the PFAS content are discussed against the measured values of organic fluorine. The third part includes an overview of commercial sludge-char's physical and chemical properties and the current legislation in the Czech Republic that allows sludge-char use on land. The total input concentration of individual PFAS and their change in quantity contained in the solid residues and acetone trapping with temperature are provided in the Supplementary Information (Additional file 1: Chapter S6 – Tables S8, S9, S10, and S11).

3.1 Artificially contaminated sea sand

Sea sand was artificially contaminated with 24 different PFASs (Additional file 1: Table S1) and pyrolyzed at a temperature ranging from 200 to 700 °C. The pyrolysis products were analyzed for 37 different PFASs (Additional file 1: Table S1), where only those PFASs added to the input were detected.

3.1.1 PFAS

3.1.1.1 Solid sample The initial PFASs contamination in sand 2,000 ± 99.7 ng g$^{-1}_{DM}$ gradually decreased to 8.3 ± 1.4 ng g$^{-1}_{DM}$ at 400 °C (Table 1 and Additional file 1: Table S8), indicating direct proportionality to temperature. The removal efficiency of the PFASs analyzed ranged from 2.2 % (200 °C) to ≥ 99.6 % at 400 °C and higher.

Of all PFASs, n-methyl-perfluoro-1-butane sulphonamide (MeFBSA) and perfluorooctane sulfonamide (FOSA) were the fastest reduced (Additional file 1: Table S8). HFPO-DA (GenX) minimizes faster than perfluorohexanoic acid (PFHxA) with the same number of perfluorinated carbons, indicating lower chain stability, probably related to the presence of a foreign group (HFPO-DA (GenX) – ether) (Sasi et al. 2021). The most thermally stable were representatives of the PFSA group, which were the only ones detected at 400 °C. The C–F and F_2CF-SO_3 bonds present in PFSAs are ranked among the strongest bonds carbon can form (Arp and Slinde 2018).

3.1.1.2 Acetone solution The PFASs' content trapped in acetone solutions shows variation with pyrolysis temperature (Table 1). The highest PFASs volatilization was observed at 400 °C. Beyond this temperature, there was a decline in the PFASs amount, indicating mineralization, decomposition into PFASs not monitored in our analysis, transformation into other organofluorinated substances (as confirmed by organic fluorine analysis), or reduced effectiveness in trapping.

In the acetone solution, only PFCAs were detected (excluding the long chain one: perfluoro-n-dodecanoic acid (PFDoA), perfluoro-n-tridecanoic acid (PFTrDA), along with perfluoro-n-tetradecanoic acid (PFTeD)), FASAs (all), and FTAs (all) (Additional file 1: Table S9). McNamara et al. (2022) proposed the PFOS degradation pathway during pyrolysis as PFOS – perfluoro-n-heptanoic acid (PFHpA) – perfluoro-n-hexanoic acid (PFHxA) – perfluoro-n-pentanoic acid (PFPeA) – PFBA. At 400 °C, when PFOS content significantly decreased, the amount of the mentioned PFCAs in acetone increased. Overall, representatives from the FASAs group were detected in the acetone solution with the highest content (Additional file 1: Table S9).

After accounting for changes in the individual PFAS contents of both pyrolysed sand and the acetone solution, along with their standard deviations, an increase in the amount of PFHxA, PFOA, PFNA, EtFOSA, and 7:3

Table 1 PFASs concentration in sand, pyrolyzed sand, acetone, and removal efficiency

		Pure sea sand	Contaminated sand	200 °C	250 °C	300 °C	400 °C	500 °C	600 °C	700 °C
Solid sample	$\Sigma24$ PFASs [ng g^{-1} $_{DM}$]	<LOQ	2,000±99.7	1,955±144	1,200±130	475±38	8.3±1.4	<LOQ	<LOQ	<LOQ
	$\Sigma24$ PFASs [ng$_{DM}$]	<LOQ	220,037±10,965	215,136±15,889	132,016±14,317	52,307±4,145	913±149	<LOQ	<LOQ	<LOQ
	PFASs removal efficiency [%]	–	–	2.2	40.0	76.2	99.6	100	100	100
Acetone	$\Sigma24$ PFASs [ng ml^{-1}]	<LOQ	–	<LOQ	4.4±0.4	7.1±0.7	11.1±2.0	3.9±0.7	<LOQ	<LOQ
	$\Sigma24$ PFASs [ng]	<LOQ	–	<LOQ	867±78	1567±157	2002±367	711±134	<LOQ	<LOQ
Total residual sum (solid sample + acetone) [ng$_{DM}$]		–	220,037±10,965	215,136±15,889	132,882±14,317	53,874±4,148	2915±396	711±134	–	–

Table 2 Average concentrations of organic fluorine in sea sand and acetone

		Pure sea sand	Contaminated sand	200 °C	250 °C	300 °C	400 °C	500 °C	600 °C	700 °C
Solid sample	Organic fluorine [ng g^{-1}$_{DW}$]	<LOQ	1585±25	1546±45	1355±81	946±7.4	37.9±8.6	42.7±6.6	25.3±3.6	16.1±2.7
	Organic fluorine [ng$_{DW}$]	<LOQ	174,363±2783	170,134±4,897	149,018±8,875	104,237±815	4127±946	4694±726	2786±396	1767±297
	Organic fluorine removal efficiency [%]	–	–	2.5	14.5	40.3	97.6	97.3	98.4	99.0
Acetone	Organic fluorine Concentration [ng ml^{-1}]	–	<LOQ	<LOQ	196±90	180±40	542±140	515±120	528±240	369±60
	Organic fluorine [ng]	–	<LOQ	<LOQ	38,681±17,762	39,450±8,767	102,329±25,354	98,906±21,952	94,739±43,063	89,135±14,493

FTA was observed at 200 °C and PFHpS at 200 °C and 300 °C (Additional file 1: Tables S8 and S9). Since the sea sand initially lacked the analysed PFAS and organofluorine before contamination (Tables 1 and 2), any observed increases can be attributed to the formation from the PFASs present. For example, PFCAs' thermal decomposition leads to forming intermediates and PFCAs with shorter chains (Sasi et al. 2021; Wang et al. 2022).

3.1.2 Organic fluorine

3.1.2.1 Solid sample The organic fluorine content of artificially contaminated sea sand decreased with increasing temperature (Table 2). However, at 250 °C and 300 °C, the organic fluorine removal rate was lower than that of analyzed PFASs (Table 1). This data suggested PFASs cleavage into non-analyzed PFASs and other organic fluorine compounds. Above 400 °C, the organic fluorine removal rate exceeded 97 %, confirming effective PFASs removal. The total fluorine removal after conversion to the inorganic state is provided in Additional file 1: Table S12.

3.1.2.2 Acetone solution The amount of organic fluorine trapped in acetone from contaminated sea sand pyrolysis increased with the temperature (Table 2). The negligible weight loss of the sand after pyrolysis (< 0.15 %) indicated a stable inorganic matrix with practically no volatiles. Consequently, the inert carrier gas contained only desorbed, pure PFAS standards and their degradation products. No condensation of the gas occurred in the instrument piping between the reactor and the impingers. Although the PFASs monitored were no longer detected at 600 °C and 700 °C (Table 1), the organofluorines (breakdown products of the PFASs analyzed) persisted in the acetone solution.

3.2 Sewage sludge

The total concentration of PFASs in the analyzed sludge was 203.9 ± 21.5 ng.g$^{-1}_{DM}$, with the highest initial concentration observed for PFOS at 166.7 ± 15.2 ng.g$^{-1}_{DM}$ (Additional file 1: Table S10). Since the Czech Republic does not have a limit for PFASs in sludge, the sludge can be used on agricultural land if the applicable legislative limits are met (see Hušek et al. (2022)). In contrast, Germany has set a PFAS limit of 100 ng.g$^{-1}_{DM}$ (the sum of PFOS and PFOA) (Röhler et al. 2021), and based on this criterion, our tested sludge would not meet the standards for use on German agricultural land.

3.2.1 PFAS

3.2.1.1 Solid samples (sludge-char) Out of 37 analyzed PFASs (Additional file 1: Table S1), 18 were detected in the sludge and pyrolysis products (Additional file 1: Table S10). The initial concentration of PFASs in the

sludge was 203.9 ± 21.5 ng.g$^{-1}_{DM}$ (Table 3), with a significant presence of PFOS (most notable), FOSA, fluorinated telomer acid (5:3) (5:3 FTA), and 8:2 FTS (Additional file 1: Table S10). The PFASs content in the sludge-char varied with increasing temperature and, at 500 °C, fell below the LOQ. A removal efficiency of over 99 % for the studied PFASs was already achieved at 400 °C.

The most stable PFAS in char was PFOS, along with representatives of the FTSAs group (fluorinated telomer sulfonate (FTS): 6:2, 8:2, and 10:2). PFOS has high thermal stability (Xiao et al. 2020). However, a significant change in content occurred in the sludge already at 200 °C, resulting in the removal of 47 % PFOS, while the remainder stayed relatively stable up to 300 °C (Additional file 1: Table S10). This PFOS behaviour contrasts with the sea sand experiments, where no significant change in PFOS content occurred below 400 °C (Additional file 1: Table S8).

We attributed this discrepancy to the different states of PFASs in the pyrolyzed material. In the sea sand experiments, PFASs were pure, adsorbed standards, whereas, in sludge, they were part of the matrix (absorbed and adsorbed) and may interact with present pollutants, microorganisms, and organic matter. Thus, a complex matrix (sludge or soil) can influence PFASs' behaviour, as Sörengård et al. (2020) observed for soil samples.

Concerning FTSAs, both 6:2 FTS and 10:2 FTS exhibited an increase in their amount compared to the original values (Additional file 1: Table S10), possibly due to their thermal stability and/or their formation from their precursors. The thermal stability of 8:2 FTS (complementing FTSAs, group), which was not present in the sludge, was previously confirmed through the pyrolysis of PFAS standards in sea sand (Additional file 1: Table S8).

3.2.1.2 Acetone solution The quantity of PFASs captured in acetone during sludge pyrolysis (Table 3) exceeded that in contaminated sand (Table 1), which initially contained nearly ten times more PFASs than the sludge. During the sludge pyrolysis, primary pyrolysis gas (a mixture of non-condensing and condensing gases) was present in piping, condensed, and trickled into impinger. PFAS could thus be captured in the condensate, along with which they entered the acetone. Conversely, the piping remained dry during sand pyrolysis.

PFASs contraction peaked at 300 °C and 400 °C. From 500 °C, there was a substantial decrease in the amount of PFAS in acetone, indicating their cleavage or mineralization. Among all the analyzed PFAS, only three were trapped in the acetone: PFHxA, FOSA, and 5:3 FTA (Additional file 1: Table S11). All three PFASs exceeded their input levels. Except for PFHxA at 200 °C, a similar increase was not observed during sand pyrolysis,

Table 3 Average concentrations of PFASs in sewage sludge, sludge-char, and acetone

		Sludge	200 °C	250 °C	300 °C	400 °C	500 °C	600 °C	700 °C
Solid sample	∑18 PFASs [ng g$^{-1}_{DM}$]	203.9 ± 21.5	119.6 ± 14.1	108.8 ± 1.7	100.4 ± 2.2	0.2 ± 0.0	< LOQ	< LOQ	< LOQ
	∑18 PFASs [ng$_{DM}$]	10,700 ± 1126	5721 ± 676	4671 ± 73	3799 ± 82	6.1 ± 0.9	< LOQ	< LOQ	< LOQ
	PFAS removal efficiency [%]	–	46.5	56.3	64.4	99.9	100	100	100
Acetone	∑18 PFASs [ng ml^{-1}]	–	4.4 ± 1.1	28.5 ± 2.5	45.7 ± 0.7	37.1 ± 6.9	27.8 ± 5.4	30.8 ± 5.1	23.7 ± 1.5
	∑18 PFASs [ng]	–	784 ± 197	5786 ± 514	9379 ± 134	8291 ± 1547	6105 ± 1194	7619 ± 1250	6941 ± 449
Total residual sum (solid sample + acetone) [ng]		10,700 ± 1126	6505 ± 704	10,457 ± 514	13,177 ± 157	8297 ± 1547	6105 ± 1194	7619 ± 1250	6941 ± 449

indicating the likely formation of these PFASs from their precursors and other unanalyzed PFAS present in the sludge.

The overall increase above the PFASs input value was observed at 300 °C, as indicated in Table 3 under the total residual sum. We attributed this phenomenon to the PFASs formation resulting from the cleavage of PFASs unanalysed and their precursors (Aro et al. 2021; Zhang et al. 2022a, b; Zhang and Liang 2021).

3.2.2 Organic fluorine content of solid samples
The organic fluorine content consistently decreased with increasing temperature, dropping from the original concentration of 62.9 ± 8.8 ng.g$^{-1}_{DM}$ to below LOQ above 400 °C (Table 4). Consequently, neither analysed PFASs nor organic fluorine were detected in our laboratory's pyrolysed sludge above 400 °C, ideally reaching 500 °C. The total fluorine removal after conversion to the inorganic state is provided in Additional file 1: Table S13.

3.2.3 Total fluorine content of condensates in acetone
The fluorine content increased with temperature and reached high levels in the acetone compared to the original organic fluorine value of the sludge (Table 4). In this context, we cannot speak specifically about organic fluorine capture but rather of total fluorine (organic and inorganic) trapped in the acetone. Unlike the sea sand, which did not contain fluorine before PFAS application, the sludge contained both fluorine forms. Organic and inorganic fluorine compounds were absorbed in condensate or/and trapped in the acetone, resulting in an increase above the input value.

3.3 WWTP Bohuslavice-Trutnov sludge-char
The commercial sludge pyrolysis unit (PYREG P500 KSF) at the WWTP Bohuslavice-Trutnov – 52,000 PE (Additional file 1: Fig. S1) was put into trial operation in 2020 and approved on October 22, 2021. Sludge is dried in a low-temperature dryer and pyrolyzed at 600 °C for at

Table 4 Average concentrations of (organic) fluorine in sewage sludge, sludge-char, and acetone

		Sludge	200 °C	250 °C	300 °C	400 °C	500 °C	600 °C	700 °C
Solid sample	Organic fluorine [ng g$^{-1}_{DM}$]	62.9 ± 8.8	48.0 ± 7.0	29.5 ± 1.1	16.7 ± 1.0	< LOQ	< LOQ	< LOQ	< LOQ
	Organic fluorine [ng$_{DM}$]	3302 ± 462	2298 ± 335	1264 ± 47	633 ± 38	< LOQ	< LOQ	< LOQ	< LOQ
	Organic fluorine removal efficiency [%]	–	30.4	61.7	80.8	> 96	100	100	100
Acetone	Fluorine [ng ml^{-1}]	–	< LOQ	320 ± 40	733 ± 20	823 ± 230	1291 ± 80	1450 ± 50	1429 ± 30
	Fluorine [ng]	–	< LOQ	64,865 ± 8108	150,404 ± 4104	183,835 ± 51,375	283,873 ± 17,591	358,655 ± 12,367	418,361 ± 8783

least 10 min. After leaving the pyrolyzer, primary pyrolysis gas is incinerated in a combustion chamber at 1000–1100 °C (Fuka et al. 2021). The annual capacity of the dryer-pyrolyzer system in use is 3,000 tonnes of mechanically dewatered sludge.

3.3.1 PFASs and organic fluorine removal
Dry sludge and sludge-char were analyzed using the same methods as the other samples tested. Of the 37 PFASs analyzed, 14 were detected. The PFASs concentration in the dry sewage sludge was 100.6 ± 12.0 ng.g^{-1} and decreased under LOQ after pyrolysis (Table 5). The results are consistent with laboratory-scale analyses: above 500 °C in char and sand, the analyzed PFASs content was below LOQ.

The organic fluorine content of the sludge was as high as PFASs, indicating the presence of other substances, such as PFASs (unanalyzed and precursors),

pharmaceuticals, or agrochemicals. After pyrolysis in a commercial unit, the sludge-char contained organic fluorine below the LOQ. The sample analyzed showed a similar behaviour to samples prepared under laboratory conditions.

3.3.2 Bohuslavice–Trutnov sludge-char: properties and legislation
The properties of the Bohuslavice–Trutnov sludge-char are listed in Table 6, and the methodology for their determination is available in Chapter 2.7. Our previous papers described the impact of temperature on sludge-char quality, including porosity and H/C ratio (Moško et al. 2021b), organic pollutants content (Moško et al. 2021a), and primary pyrolysis gas energy yield (Moško et al. 2020). Temperatures above 500 °C (ideally at the rated output above 600 °C) can be considered sufficient to influence all these variables positively.

Table 5 PFASs content in dry sludge and sludge-char from Bohuslavice-Trutnov WWTP (in dry matter)

	PFPeA	PFHxA	PFHpA	PFOA	PFNA	PFDA	PFUdA
Dry sewage sludge [ng g^{-1}$_{DM}$]	2.3 ± 0.2	9.2 ± 0.6	1.5 ± 0.3	0.7 ± 0.9	2.7 ± 0.1	8.0 ± 1.9	5.3 ± 1.5
Sludge-char [ng g^{-1}$_{DM}$]	< LOQ	< LOQ	< LOQ	< LOQ	< LOQ	< LOQ	< LOQ
	PFDoA	PFTrDA	PFTeDA	PFHpS	PFOS	5:3 FTA	10:2 FTS
Dry sewage sludge [ng g^{-1}$_{DM}$]	12.5 ± 0.2	4.9 ± 0.4	4.4 ± 0.3	2.9 ± 0.7	11.7 ± 0.3	32.5 ± 14.3	1.9 ± 0.2
Sludge-char [ng g^{-1}$_{DM}$]	< LOQ	< LOQ	< LOQ	< LOQ	< LOQ	< LOQ	< LOQ
∑ PFASs$_{14}$ in sewage sludge [ng g^{-1}$_{DM}$]		100.6 ± 12.0					
∑ PFASs in sludge-char [ng g^{-1}$_{DM}$]		< LOQ					
Organic fluorine concentration in sludge [ng g^{-1}$_{DM}$]		100.5 ± 9.1					
Organic fluorine concentration in sludge-char[ng g^{-1}$_{DM}$]		< LOQ					

Table 6 Properties of sludge-char from Bohuslavice-Trutnov WWTP (in dry matter)

Process temperature [°C]					
600 °C					
S$_{BET}$ [m^2 g^{-1}]	S$_{meso}$ [m^2 g^{-1}]	V$_{tot}$ [mm^3$_{liq}$ g^{-1}]	V$_{micro}$ [mm^3$_{liq}$ g^{-1}]	V$_{intr}$ [cm^3 g^{-1}]	ρ_{Hg} [g cm^{-3}]
45.0	21.0	61.0	13.0	0.42	1.03
ρ_{He} [g cm^{-3}]	ε [–]	A [wt%]	C [wt%]	H [wt%]	N [wt%]
2.29	0.55	76.2	22.3	0.50	1.46
S [wt%]	H/C	Sum 16 PAH [mg kg^{-1}]	Sum PCB [mg kg^{-1}]	Sum PPCP [mg kg^{-1}]	P$_2$O$_5$ [wt%]
0.70	0.27	< 0.50	< 0.01	LOQ	9.30

S$_{BET}$, Specific surface area; S$_{meso}$, Specific surface area of mesopores; V$_{tot}$, Total pore volume; V$_{micro}$, Microporesvolume; ρ_{Hg}, Apparent density; ρ_{He}, True solid density; ε, porosity determined as $\varepsilon = 1 - (\rho_{Hg}/\rho_{He})$; A, Ash; H/C, Hydrogen to Carbon molar ratio; Sum 16 PAH, sum of acenaphthene, acenaphthylene, anthracene, benzo(a) anthracene, benzo(a)pyrene, benzo(b)fluoranthene, benzo(g,h,i)perylene, benzo(k)fluoranthene, chrysene, dibenz(a,h), fluorene, fluoranthene, indeno(1,2,3-c,d) pyrene, naphthalene, phenanthrene, and pyrene; PCBs, sum of 7 congeners: 28 + 52 + 101 + 118 + 138 + 153 + 180; PPCP, sum of 17alpha-Estradiol, 17beta-Estradiol, Acesulfame, Acetaminophen (Paracetamol), Amitriptyline, Atenolol, Atorvastatin, Bisphenol A (BPA), Bisphenol F (BPF), Caffeine, Carbamazepine, Carbamazepine 10,11-epoxide, Cetirizine, Citalopram, Clarithromycin, Daidzein, Diclofenac, Equilin, Equol, Erythromycin, Estriol, Estrone, Ethinylestradiol, Fluconazole, Furosemide, Gabapentin, Genistein, Hydrochlorothiazide, Ibuprofen, Iomeprol, Ketoprofen, Lamotrigine, Metoprolol, Mirtazapine, Naproxen, Norethindrone, Norgestrel, Omeprazole, Paraxanthine, Saccharine, Sulfamethazine, Sulfamethoxazole, Sulfanilamide, Sulfapyridine, Telmisartan, Tramadol, Triclosan, Trimethoprim, Venlafaxine, Zearalenol

Table 7 Czech legislative pollutants limits for sludge-char used in agriculture land and their content in sludge-char produced at the Bohuslavice-Trutnov WWTP (in dry matter) (Regulation No. 474/2000 Coll.)

	Cd	Pb	Hg	As	Cr	Sum 12 PAH
CZE legislative limits [mg kg$^{-1}_{DM}$]	5.00	100	0.50	30.0	100	20.0
Bohuslavice WWTP sludge-char [mg kg$^{-1}_{DM}$]	0.46	57.2	0.003	2.94	74.1	< 0.50

Sum 12 PAH, sum of anthracene, benzo(a)anthracene, benzo(b)fluoranthene

benzo(k)fluoranthene, benzo(a)pyrene, benzo(ghi)perylene, phenanthrene, fluoranthene, chrysene, indeno(1,2,3–cd)pyrene, naphthalene, and pyrene

Regarding European Union legislation, the use of sludge-char as a soil improver is currently not supported due to the lack of information on removing organic pollutants (Huygens et al. 2019; Regulation (EU) 2019/1009). However, this regulation does not impact the internal markets of the Member States (Regulation (EU) 2019/1009). In the Czech Republic, the legislation on fertilizers changed on November 1, 2021, (Regulation No. 474/2000 Coll. 2021), and the use of sludge-char on land becomes possible if the legislative limits are met (Table 7), the char obtains necessary registration, and end-of-waste status.

Sludge-char from Bohuslavice-Trutnov WWTP was registered as a soil improver by the Central Institute for Supervising and Testing in Agriculture of the Czech Republic on March 7, 2022 (UKZUZ 2022). On July 4, 2022, the regional authority removed Bohuslavice sludge-char from the waste catalogue and transferred it to the end-of-waste status (KUKHK 2022).

4 Conclusion

Pyrolysis at 400 °C and above effectively removes monitored PFASs, a finding validated under both laboratory and operational conditions. Conversely, torrefaction and pyrolysis below 400 °C are unsuitable for PFASs removal. Due to the large number of different PFASs, it is advisable to include the analysis of organic fluorine. Organic fluorine includes all PFASs, regardless of functional group, and other fluorine-containing substances such as agrochemicals and certain pharmaceuticals. In our experiments, the organic fluorine content was significantly removed from solid samples from 400 °C onwards, which is in line with the results for PFASs removal.

The amount of PFASs and organic fluorine also changed with temperature in the primary pyrolysis gas trapped in acetone, indicating the capability to evaporate at the expense of the remaining content in the char and sand. This was combined with the short residence time of the primary pyrolysis gas, which was insufficient to destroy the PFASs inside the reactor. Based on these facts, in commercial sludge pyrolysis units, in addition to sufficient heat and appropriate reactor design

(residence time), the produced gas must be cleaned or treated in a combustion chamber where the remaining PFASs, organic fluorine, and other organics are oxidized (decomposed).

Due to the diverse range of contaminants, including PFASs, and the sludge-char quality, the minimum operating temperature of a commercial sludge pyrolysis unit should be above 500 °C at a rated output above 600 °C and the residence time of the sludge/sludge-char in the pyrolyzer should be at least 10 min. The resultant sludge-char can be used as a soil improver but will always contain a certain amount of heavy metals concentrated from the sludge. Therefore, usage should be restricted to areas outside of food production, such as land reclamation, green areas, and parks. Further research directions should lead to verifying our results by measuring organic fluorine in other commercial sludge pyrolysis units operating under the above-mentioned conditions and starting a discussion on setting limits for organic fluorine as a new general limit for waste-based materials.

Supplementary Information

The online version contains supplementary material available at https://doi.org/10.1007/s42773-024-00322-5.

Additional file 1: Figure S1. Map with the location of WWTP Bohuslavice (map source: Mapy.cz). **Figure S2.** FTIR analysis of sewage sludge and sludge-char. **Figure S3.** Main gaseous species in non-condensable pyrolysis gas. **Table S1.** Summary of analysed PFASs (asterisked artificial contaminants for sea sands). **Table S2.** Selected physical and chemical properties of sewage sludge (in dry matter). **Table S3.** Elementary analysis of sewage sludge. **Table S4a.** Detailed settings of the mass spectrometer and limits of detection/quantification. **Table S4b**. Detailed settings of the mass spectrometer and limits of detection/quantification. **Table S5.** Mass balance of the sludge pyrolysis and distribution of energy of the sludge among the products. **Table S6.** Complex compositions of non-condensable pyrolysis gas. **Table S7.** Main gaseous sulphur compounds in non-condensable pyrolysis gas; expressed as a gram of S per m^{-3}. **Table S8.** PFASs concentration [ng.g.$^{-1}$] and amount [ng] in sea sand and pyrolyzed sand (average). **Table S9.** PFASs amount [ng] in acetone from artificially contaminated sea sand pyrolysis (average). **Table S10.** PFASs concentration [ng.g.$^{-1}$] and amount [ng] in sewage sludge and sludge char (average). **Table S11.** PFASs amount [ng] in acetone from sewage sludge pyrolysis (average). **Table S12.** Change in total fluorine content of sea sand samples. **Table S13.** Change in total fluorine content of sewage sludge samples. **Table S14.** Total fluorine content – pyrolysis unit Bohuslavice Trutnov WWTP.

Declarations

Competing interests

The authors have no relevant financial or non-financial interests to disclose.

Author details

[1]Institute of Chemical Process Fundamentals, The Czech Academy of Sciences, Rozvojová 1/135, Suchdol, 165 00 Prague 6, Czech Republic. [2]Department of Power Engineering, Faculty of Environmental Technology, University of Chemistry and Technology, Prague, Technická 5, 166 28 Prague 6, Czech Republic. [3]Institute of Microbiology, The Czech Academy of Sciences, Vídeňská 1083, 142 20 Prague 4, Czech Republic. [4]Department of Sustainable Fuels and Green Chemistry, Faculty of Environmental Technology, University of Chemistry and Technology, Prague, Technická 5, 166 28 Prague 6, Czech Republic. [5]Institute for Environmental Studies, Faculty of Science, Charles University, Benátská 2, 128 01 Prague 2, Czech Republic. [6]Department of Environmental Geosciences, Faculty of Environmental Sciences, Czech University of Life Sciences Prague, Kamýcká 129, Suchdol, 165 00 Prague, Czech Republic.

References

Alinezhad A, Challa Sasi P, Zhang P, Yao B, Kubátová A, Golovko SA, Golovko MY, Xiao F (2022) An investigation of thermal air degradation and pyrolysis of per- and polyfluoroalkyl substances and aqueous film-forming foams in soil. ACS EST Eng 2:198–209. https://doi.org/10.1021/acsestengg.1c00335

Aro R, Eriksson U, Kärrman A, Chen F, Wang T, Yeung LWY (2021) Fluorine mass balance analysis of effluent and sludge from Nordic countries. ACS EST Water 1:2087–2096. https://doi.org/10.1021/acsestwater.1c00168

Arp PH, Slinde AG (2018) PFBS in the environment: monitoring and physical-chemical data related to the environmental distribution of perfluorobutanesulfonic acid. Norwegian geotechnical institute, Olso. https://www.miljodirektoratet.no/globalassets/publikasjoner/M1122/M1122.pdf

Ateia M, Maroli A, Tharayil N, Karanfil T (2019) The overlooked short- and ultra-short-chain poly- and perfluorinated substances: a review. Chemosphere 220:866–882. https://doi.org/10.1016/j.chemosphere.2018.12.186

Bamdad H, Papari S, Moreside E, Berruti F (2022) High-temperature pyrolysis for elimination of per- and polyfluoroalkyl substances (PFAS) from biosolids. Processes 10:2187. https://doi.org/10.3390/pr10112187

Buck RC, Franklin J, Berger U, Conder JM, Cousins IT, de Voogt P, Jensen AA, Kannan K, Mabury SA, van Leeuwen SP (2011) Perfluoroalkyl and polyfluoroalkyl substances in the environment: terminology, classification, and origins. Integr Environ Assess Manag 7:513–541. https://doi.org/10.1002/ieam.258

Buss W (2021) Pyrolysis solves the issue of organic contaminants in sewage sludge while retaining carbon—making the case for sewage sludge treatment via pyrolysis. ACS Sustain Chem Eng 9:10048–10053. https://doi.org/10.1021/acssuschemeng.1c03651

EPA (2021) PFAS master list of PFAS substances. CompTox chemicals dashboard. https://comptox.epa.gov/dashboard/chemical-lists/pfasmaster. Accessed 6 June 2024

Fenton SE, Ducatman A, Boobis A, DeWitt JC, Lau C, Ng C, Smith JS, Roberts SM (2021) Per- and polyfluoroalkyl substance toxicity and human health review: current state of knowledge and strategies for informing future research. Environ Toxicol Chem 40:606–630. https://doi.org/10.1002/etc.4890

Fuka J, Kos M, Pohořelý M (2021) Drying and pyrolysis at Trutnov WWTP—the first results of test operation [Sušení a pyrolýza na ČOV Trutnov—první výsledky zkušebního provozu]. SOVAK 30:24–28

Ghisi R, Vamerali T, Manzetti S (2019) Accumulation of perfluorinated alkyl substances (PFAS) in agricultural plants: a review. Environ Res 169:326–341. https://doi.org/10.1016/j.envres.2018.10.023

Glüge J, Scheringer M, Cousins IT, DeWitt JC, Goldenman G, Herzke D, Lohmann R, Ng CA, Trier X, Wang Z (2020) An overview of the uses of per- and polyfluoroalkyl substances (PFAS). Environ Sci Process Impacts. 22:2345–2373. https://doi.org/10.1039/D0EM00291G

Hall H, Moodie D, Ver C (2021) PFAS in biosolids: a review of international regulations. Water e-Journal. https://doi.org/10.21139/wej.2020.026

Han J, Kiss L, Mei H, Remete AM, Ponikvar-Svet M, Sedgwick DM, Roman R, Fustero S, Moriwaki H, Soloshonok VA (2021) Chemical aspects of human and environmental overload with fluorine. Chem Rev 121:4678–4742. https://doi.org/10.1021/acs.chemrev.0c01263

Horst J, McDonough J, Ross I, Houtz E (2020) Understanding and Managing the potential by-products of PFAS destruction. Groundw Monit Remediat 40:17–27. https://doi.org/10.1111/gwmr.12372

Hušek M, Moško J, Pohořelý M (2022) Sewage sludge treatment methods and P-recovery possibilities: current state-of-the-art. J Environ Manage 315:115090. https://doi.org/10.1016/j.jenvman.2022.115090

Huygens D, Delgado Sancho L, Saveyn HGM, Tonini D, Eder P, European Commission, Joint Research Centre (2019). Technical proposals for selected new fertilising materials under the Fertilising Products Regulation (Regulation (EU) 2019/1009): process and quality criteria, and assessment of environmental and market impacts for precipitated phosphate salts and derivates, thermal oxidation materials and derivates and pyrolysis and gasification materials

Kärrman A, Yeung LW, Spaan KM, Lange FT, Nguyen MA, Plassmann M, de Wit CA, Scheurer M, Awad R, Benskin JP (2021) Can determination of extractable organofluorine (EOF) be standardized? First interlaboratory comparisons of EOF and fluorine mass balance in sludge and water matrices. Environ Sci Process Impacts 23:1458–1465. https://doi.org/10.1039/D1EM00224D

Kotthoff M, Bücking M (2018) Four chemical trends will shape the next decade's directions in perfluoroalkyl and polyfluoroalkyl substances research. Front Chem. 6:103

KUKHK (2022) Decree KUKHK—17763/ZP/2022/Le/8 [Rozhodnutí KUKHK – 17763/ZP/2022/Le/8]

Kundu S, Patel S, Halder P, Patel T, Marzbali MH, Kumar Pramanik B, Paz-Ferreiro J, de Figueiredo CC, Bergmann D, Surapaneni A, Megharaj M, Shah K (2021) Removal of PFASs from biosolids using a semi-pilot scale pyrolysis reactor and the application of biosolids derived biochar for the removal

of PFASs from contaminated water. Environ Sci Water Res Technol 7:638–649. https://doi.org/10.1039/D0EW00763C

Mancinelli E, Baltrėnaitė E, Baltrėnas P, Paliulis D, Passerini G (2016) Trace metals in biochars from biodegradable by-products of industrial factors. Water Air Soil Pollut 227:198. https://doi.org/10.1007/s11270-016-2892-1

McNamara P, Samuel MS, Sathyamoorthy S, Moss L, Valtierra D, Lopez HC, Nigro N, Somerville S, Liu Z (2022) Pyrolysis transports, and transforms, PFAS from biosolids to py-liquid. Environ Sci Water Res Technol. https://doi.org/10.1039/D2EW00677D

Moško J, Pohořelý M, Skoblia S, Beňo Z, Jeremiáš M (2020) Detailed analysis of sewage sludge pyrolysis gas: effect of pyrolysis temperature. Energies 13:4087. https://doi.org/10.3390/en13164087

Moško J, Pohořelý M, Cajthaml T, Jeremiáš M, Robles-Aguilar AA, Skoblia S, Beňo Z, Innemanová P, Linhartová L, Michalíková K, Meers E (2021a) Effect of pyrolysis temperature on removal of organic pollutants present in anaerobically stabilized sewage sludge. Chemosphere 265:129082. https://doi.org/10.1016/j.chemosphere.2020.129082

Moško J, Pohořelý M, Skoblia S, Fajgar R, Straka P, Soukup K, Beňo Z, Farták J, Bičáková O, Jeremiáš M, Šyc M, Meers E (2021b) Structural and chemical changes of sludge derived pyrolysis char prepared under different process temperatures. J Anal Appl Pyrolysis. https://doi.org/10.1016/j.jaap.2021.105085

Moško J, Jeremiáš M, Skoblia S, Beňo Z, Sikarwar VS, Hušek M, Wang H, Pohořelý M (2022) Residual moisture in the sewage sludge feed significantly affects the pyrolysis process: Simulation of continuous process in a batch reactor. J Anal Appl Pyrolysis. https://doi.org/10.1016/j.jaap.2021.105387

Munoz G, Michaud AM, Liu M, Vo Duy S, Montenach D, Resseguier C, Watteau F, Sappin-Didier V, Feder F, Morvan T, Houot S, Desrosiers M, Liu J, Sauvé S (2022) Target and nontarget screening of PFAS in biosolids, composts, and other organic waste products for land application in france. Environ Sci Technol 56:6056–6068. https://doi.org/10.1021/acs.est.1c03697

O'Hagan D (2008) Understanding organofluorine chemistry: an introduction to the C–F bond. Chem Soc Rev 37:308–319. https://doi.org/10.1039/B711844A

Regulation (EU) 2019/1009 of the European Parliament and of the Council of 5 June 2019 laying down rules on the making available on the market of EU fertilising products and amending Regulations (EC) No 1069/2009 and (EC) No 1107/2009 and repealing Regulation (EC) No 2003/2003 (consolidated version: 16 March 2023 October 2022), 2023

Regulation No. 474/2000 (2021) Coll. of the Ministry of Agriculture on the specification of requirements for fertilisers [Vyhláška Ministerstva zemědělství č. 474/2000 Sb., o stanovení požadavků na hnojiva] (consolidated version 01 November 2021)

Röhler K, Haluska AA, Susset B, Liu B, Grathwohl P (2021) Long-term behavior of PFAS in contaminated agricultural soils in Germany. J Contam Hydrol 241:103812. https://doi.org/10.1016/j.jconhyd.2021.103812

Ruan T, Lin Y, Wang T, Liu R, Jiang G (2015) Identification of novel polyfluorinated ether sulfonates as PFOS alternatives in municipal sewage sludge in China. Environ Sci Technol 49:6519–6527. https://doi.org/10.1021/acs.est.5b01010

Sasi PC, Alinezhad A, Yao B, Kubátová A, Golovko SA, Golovko MY, Xiao F (2021) Effect of granular activated carbon and other porous materials on thermal decomposition of per- and polyfluoroalkyl substances: Mechanisms and implications for water purification. Water Res 200:117271. https://doi.org/10.1016/j.watres.2021.117271

Semerád J, Hatasová N, Grasserová A, Černá T, Filipová A, Hanč A, Innemanová P, Pivokonský M, Cajthaml T (2020) Screening for 32 per- and polyfluoroalkyl substances (PFAS) including GenX in sludges from 43 WWTPs located in the Czech Republic—evaluation of potential accumulation in vegetables after application of biosolids. Chemosphere 261:128018. https://doi.org/10.1016/j.chemosphere.2020.128018

Semerád J, Horká P, Filipová A, Kukla J, Holubová K, Musilová Z, Jandová K, Frouz J, Cajthaml T (2022) The driving factors of per- and polyfluorinated alkyl substance (PFAS) accumulation in selected fish species: The influence of position in river continuum, fish feed composition, and pollutant properties. Sci Total Environ. https://doi.org/10.1016/j.scitotenv.2021.151662

Sörengård M, Lindh A-S, Ahrens L (2020) Thermal desorption as a high removal remediation technique for soils contaminated with per- and

polyfluoroalkyl substances (PFASs). PLoS ONE 15:e0234476. https://doi.org/10.1371/journal.pone.0234476

Sørmo E, Castro G, Hubert M, Licul-Kucera V, Quintanilla M, Asimakopoulos AG, Cornelissen G, Arp HPH (2023) The decomposition and emission factors of a wide range of PFAS in diverse, contaminated organic waste fractions undergoing dry pyrolysis. J Hazard Mater 454:131447. https://doi.org/10.1016/j.jhazmat.2023.131447

Stahl T, Mattern D, Brunn H (2011) Toxicology of perfluorinated compounds. Environ Sci Eur 23:38. https://doi.org/10.1186/2190-4715-23-38

Tavasoli E, Luek JL, Malley JP, Mouser PJ (2021) Distribution and fate of per- and polyfluoroalkyl substances (PFAS) in wastewater treatment facilities. Environ Sci Process Impacts. 23:903–913. https://doi.org/10.1039/D1EM00032B

Thoma ED, Wright RS, George I, Krause M, Presezzi D, Villa V, Preston W, Deshmukh P, Kauppi P, Zemek PG (2022) Pyrolysis processing of PFAS-impacted biosolids, a pilot study. J Air Waste Manag Assoc 72:309–318. https://doi.org/10.1080/10962247.2021.2009935

UKZUZ (2022) Decree UKZUZ—R12026 [Rozhodnutí UKZUZ—R12026]

Wang J, Lin Z, He X, Song M, Westerhoff P, Doudrick K, Hanigan D (2022) Critical review of thermal decomposition of per- and polyfluoroalkyl substances: mechanisms and implications for thermal treatment processes. Environ Sci Technol 56:5355–5370. https://doi.org/10.1021/acs.est.2c02251

Weber NH, Stockenhuber SP, Delva CS, Abu Fara A, Grimison CC, Lucas JA, Mackie JC, Stockenhuber M, Kennedy EM (2021) Kinetics of decomposition of PFOS relevant to thermal desorption remediation of soils. Ind Eng Chem Res 60:9080–9087. https://doi.org/10.1021/acs.iecr.1c01504

Williams T, Grieco S, Bani B, Friedenthal A, White A (2021) Removal and transformation of PFAS from biosolids in a high temperature pyrolysis system: a bench scale evaluation. Residuals Biosolids Conf. https://doi.org/10.2175/193864718825157943

Winchell LJ, Ross JJ, Wells MJM, Fonoll X, Norton JW, Bell KY (2021) Per- and polyfluoroalkyl substances thermal destruction at water resource recovery facilities: a state of the science review. Water Environ Res 93:826–843. https://doi.org/10.1002/wer.1483

Xiao F, Sasi PC, Yao B, Kubátová A, Golovko SA, Golovko MY, Soli D (2020) Thermal stability and decomposition of perfluoroalkyl substances on spent granular activated carbon. Environ Sci Technol Lett 7:343–350. https://doi.org/10.1021/acs.estlett.0c00114

Zhang W, Liang Y (2021) Effects of hydrothermal treatments on destruction of per- and polyfluoroalkyl substances in sewage sludge. Environ Pollut 285:117276. https://doi.org/10.1016/j.envpol.2021.117276

Zhang Z, Ju R, Zhou H, Chen H (2021) Migration characteristics of heavy metals during sludge pyrolysis. Waste Manage 120:25–32. https://doi.org/10.1016/j.wasman.2020.11.018

Zhang W, Jiang T, Liang Y (2022a) Stabilization of per- and polyfluoroalkyl substances (PFAS) in sewage sludge using different sorbents. J Hazard Mater Adv 6:100089. https://doi.org/10.1016/j.hazadv.2022.100089

Zhang Z, Sarkar D, Biswas JK, Datta R (2022b) Biodegradation of per- and polyfluoroalkyl substances (PFAS): a review. Biores Technol 344:126223. https://doi.org/10.1016/j.biortech.2021.126223